

# Electrochemical dissolution of tungsten under pulsed conditions

A. D. DAVYDOV, V. S. SHALDAEV, A. N. MALOFEEVA, I. V. SAVOTIN

*Frumkin Institute of Electrochemistry, Russian Academy of Sciences, Moscow, 117071*

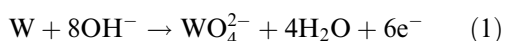
Received 8 January 1996; revised 22 July 1996

Limiting diffusion currents for the anodic dissolution of a tungsten rotating disc electrode in alkaline solution under rectangular current pulses have been determined experimentally. These currents were calculated by use of approaches developed by Ib1, Cheh, and Chin. Experimental and calculated results were compared. It is shown that the use of bipolar voltage pulses enhanced the anodic dissolution of tungsten in alkaline medium.

## 1. Introduction

In aqueous solutions, a  $\text{WO}_3$  anodic film, which passivates the metal and hinders its dissolution, is formed on tungsten surfaces. This film is highly soluble only in alkaline solutions; therefore, a high rate of electrochemical dissolution of tungsten occurs only in these solutions. Consequently, all processes, which are based on the anodic dissolution of tungsten and are of practical importance, are conducted in alkaline solutions. This is true for electrochemical machining, electrochemical polishing and etching, and the processing of metal tungsten scrap.

The anodic dissolution of tungsten proceeds according to the following overall reaction:



The rate of this reaction is restricted by the limiting current  $i_l$ ; in the region of  $i_l$ , an oxide film is present at the anode surface. The thickness of the film is determined by the anodic potential, concentration of alkali, hydrodynamic conditions, and electrolyte temperature [1]. The limiting current condition is characterized by the equality between the rates of oxide film formation (the intermediate stages of Reaction 1) and of its dissolution with the formation of tungstate, which is the end product of the reaction.

In earlier papers [2, 3], the theory of mass transfer was developed for the processes of anodic metal dissolution involving electrolyte anions under steady-state conditions. On the basis of this theory, the following equation for calculating  $i_l$  of Reaction 1 was derived and confirmed experimentally [4]:

$$i_l = \frac{0.114 nFD_1c_0}{\delta} \quad (2)$$

where  $D_1$  and  $D_2$  are the diffusion coefficients of ions  $\text{OH}^-$  and  $\text{WO}_4^{2-}$ , respectively,  $n$  is the number of electrons involved in Reaction 1,  $c_0$  is the bulk concentration of anions, and  $\delta$  is the thickness of the diffusion boundary layer. The thickness  $\delta$  may be calculated by the Levich equation:

$$\delta = 1.61 D_1^{1/3} \nu^{1/6} \omega^{-1/2} \quad (3)$$

where  $\nu$  is the solution kinematic viscosity. In the present study we have measured and calculated the limiting currents of tungsten dissolution under rectangular current pulses.

## 2. Procedure

The studies were performed using an RDE at a rotation rate of 700 rpm in 2.564 M NaOH solution. A PI-50-1 potentiostat-galvanostat with a PR-8 programmer was used. The pulse limiting current  $i_{lp}$  (the current density, at which the near-electrode concentration of  $\text{OH}^-$  ions decreases to zero at the end of the pulse) was determined in the following way. The amplitude of square current pulses was gradually increased and the potential pulses were recorded by oscillograph until a jumpwise increase in signal began at the end of the pulse. In all experiments, more than 20 pulses were applied.

In a specific set of experiments, the potential pulses of various amplitude and duration were applied, and the corresponding current pulses were recorded. In this case, some experiments were performed under the condition that, in the pauses between the anodic pulses, a potential was set at which the current was not recorded (unipolar potential pulses). In other experiments, in the pauses between the anodic potential pulses, cathodic potential pulses were applied with a given amplitude (bipolar pulses). Current consumed by the electrical double layer, was not taken into account, since it is very small.

## 3. Calculation of pulse limiting current

Several approaches to the theoretical description of mass transfer in electrochemical processes under pulse conditions are possible [5–10]. All were developed within the framework of the theory of dilute solutions, without regard for the migration mechanism of ion transfer. The calculations of  $i_{lp}$  were con-

ducted for the cathodic deposition of metals [11–15] and for the oxidation–reduction reaction [16].

In this study three approaches were used for calculating  $i_{ip}$  for the anodic dissolution of metal. The first was the model approach of Ibl [8, 9], who proposed that there are two diffusion near-electrode layers. The thickness of the stationary (outer) diffusion layer,  $\delta$ , is time-invariant and may be calculated by the method of the theory of steady-state convective diffusion. The thickness of the pulse (inner) diffusion layer,  $\delta_p$ , varies with time with the frequency of the pulse current.

The pulse limiting current is as follows:

$$i_{ip} = nFDc^*/\delta_p \quad (4)$$

where  $c^*$  is the reagent concentration at the interface between the stationary and pulse diffusion layers. By considering ion transfer in both diffusion layers within the framework of this model, an expression for  $i_{ip}$  involving no  $c^*$  term was obtained:

$$i_{ip} = i_l \left[ \frac{\delta_p}{\delta} (1 - \gamma) + \gamma \right]^{-1} \quad (5)$$

where  $t_1$  and  $t_2$  are the pulse-on and pulse-off times, respectively,  $\gamma = t_1 / (t_1 + t_2)$ . (The equation for  $i_{ip}$  in this form is presented in [12]).

According to Ibl, the thickness  $\delta_p$  is determined as follows:

$$\delta_p = \{2D_1 t_1 (1 - \gamma)\}^{1/2} \quad (6)$$

From Equation 5 it follows that at a high  $\gamma$  (close to unity),  $i_{ip} \approx i_l$ . At a low  $\gamma$  (much less than unity),  $i_{ip} \approx i_l (\delta_p/\delta)^{-1}$ , i.e. the difference between  $i_{ip}$  and  $i_l$  is essentially determined by  $t_1$  (see Equation 6).

In parallel with calculating  $i_{ip}$  according to Ibl, we used Cheh's equation [11], which is derived on the basis of solution of the problem of nonsteady-state mass transfer obtained by Rosebrugh and Miller [5]. By analogy with Equation 5, this may be written as

$$i_{ip} = i_l \left[ 1 - \frac{8}{\pi^2} \sum_{j=1}^{\infty} \frac{1}{b} \times \frac{(\exp[abt_2] - 1)}{(\exp[ab(t_1 + t_2)] - 1)} \right]^{-1} \quad (7)$$

where  $a = \pi^2 D_1 / 4\delta^2$ ,  $b = (2j - 1)^2$ ,  $j$  is an integer. Chin's solution of the problem of nonsteady-state convective mass transfer for the rectangular pulse current leads to the equation for  $i_{ip}$  [14], which may be written as

$$i_{ip} = i_l \left[ \frac{2}{\pi^2} \sum_{j=1}^{\infty} \frac{1 - \exp(-\lambda\gamma)}{(j - 1/2)^2 [1 - \exp(-\lambda)]} \right]^{-1} \quad (8)$$

where  $\lambda = \pi^2 D_1 (t_1 + t_2) (j - 1/2)^2 / \delta^2$ ;  $\delta$  is determined by Equation 3.

#### 4. Experimental and calculated results

To calculate  $i_{ip}$ , it is, first necessary to determine  $i_l$ . For this purpose, Equations 2 and 3 were used with  $c_0 = 2.564 \times 10^{-3} \text{ mol cm}^{-3}$ ,  $D_1 = 5.26 \times 10^{-5} \text{ cm}^2 \text{ s}^{-1}$ ,  $\nu = 10^{-2} \text{ cm}^2 \text{ s}^{-1}$ ,  $\omega = 2\pi m$ , where  $m = 11.66 \text{ rps}$ .

We obtained:  $i_l = 2.74 \text{ A cm}^{-2}$ . In a set of pulse experiments, the measurements and calculations were performed at a constant pulse-on time  $t_1 = 2 \times 10^{-3} \text{ s}$  and various  $t_2$  (Fig. 1(a)). In another set of experiments, the measurements and calculations were performed at a constant pulse-on time  $t_1 = 1 \times 10^{-1} \text{ s}$  (Fig. 1(b)).

Figure 1 shows the plots of  $i_{ip}$  against  $\gamma$ , obtained experimentally (crosses) and calculated by Equations 5 (circles), 7 (triangles) and 8 (squares). The value of the steady-state limiting current  $i_l$  is given by a dotted line. We put  $j = 5$  for Equation 7 and  $j = 10000$  for Equation 8.

It may be seen from Fig. 1 that all results, obtained at high  $\gamma$  values ( $\gamma \geq 0.5$ ), agree closely; at  $\gamma \approx 1$ , as expected,  $i_{ip}$  is virtually coincident with  $i_l$ . At low  $\gamma$ , the results of  $i_{ip}$ , calculated by Equations 7 and 8, agree very closely (this is favoured by the possibility for choosing the most suitable values of  $j$ ) and give  $i_{ip}$  values which are higher than those calculated by Equation 5 at both values of  $t_1$ . This may be associated with a difference in physical models, which form the basis of various approaches to the  $i_{ip}$  calculation. Model [8, 9] is very descriptive but less rigorous. At low  $\gamma$ , the experimental data on pulse

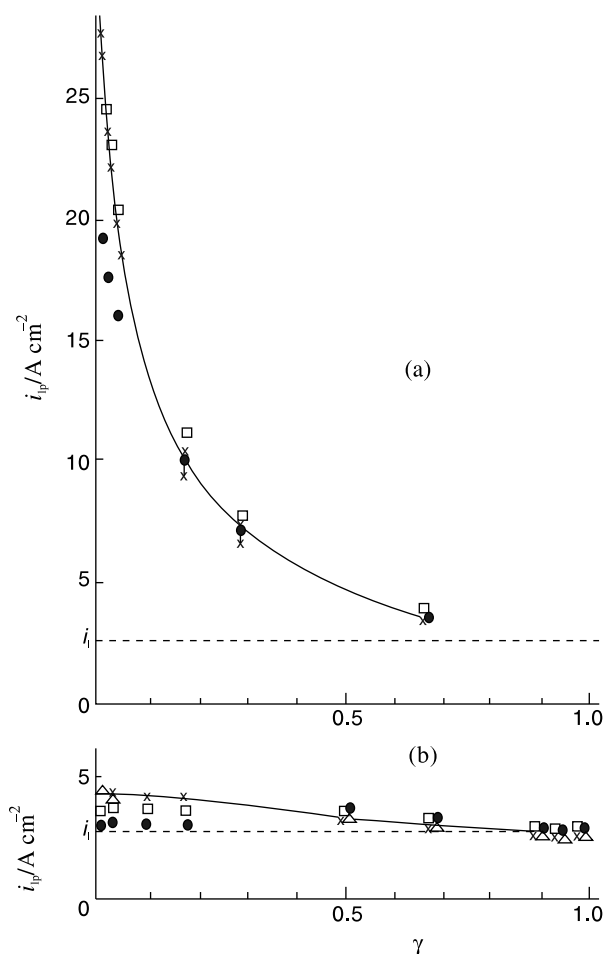


Fig. 1. Plots of limiting pulse current,  $i_{ip}$ , of anode dissolution of a tungsten RDE against  $\gamma$  at (a)  $t_1 = 2 \times 10^{-3} \text{ s}$  and (b)  $t_1 = 1 \times 10^{-1} \text{ s}$ . Key: (x) measured values; (●, △, □) calculated values for Equations 5, 7, 8, respectively.

anodic dissolution of tungsten in alkali are better described by Equations 7 and 8. The deviation of calculated  $i_{lp}$  values from experimental values usually lies within 10%.

In [11] it was shown that an average limiting diffusion current under pulse conditions ( $\bar{i}_{lp} = i_{lp}\gamma$ ) does not exceed the steady-state limiting current  $i_l$ . In this respect, the productivity of pulse electrolysis may be only equal to, or lower than, the productivity of electrolysis under direct-current conditions. Our experimental data is in accordance with this proposition. For example, at  $t_1 = 1 \times 10^{-1}$  s,  $\bar{i}_{lp}$  increases from  $0.03 i_l$  to  $0.99 i_l$  with increase in  $\gamma$  from 0.02 to 0.99.

In some cases, application of *bipolar* pulse operating conditions, may raise the process productivity as compared with *unipolar* pulses. This may be demonstrated with the anodic dissolution of tungsten in alkaline medium. In this system, water electrolysis proceeds with hydrogen evolution during the cathodic polarization. In a set of experiments, pulses of anodic potential  $E_a$  with increasing amplitude were applied in the unipolar regime, and in another set of experiments they were applied in the bipolar regime (amplitude of cathodic pulse  $E_c = 2$  V (Ag/AgCl, sat. KCl), and the responses of anodic current were recorded. Figure 2 gives the plots of current density at the end of the anodic pulse versus amplitude,  $E_a$ , of the potential applied for both sets of experiments.

In the first set, the current density at the end of the pulse does not increase with increase in  $E_a$  (although, at the beginning of the pulse, the higher the value of  $E_a$ , the higher is the current density) and is virtually equal to  $i_l$ . Obviously, the near-electrode concentration of hydroxyl ions,  $c_s$ , decreases to zero by the end of pulse at any  $E_a$  used (and also  $t_1$  and  $t_2$ ). In the second case, the current density at the end of the pulse increases approximately linear with  $E_a$ . The rate of anodic tungsten dissolution may be increased

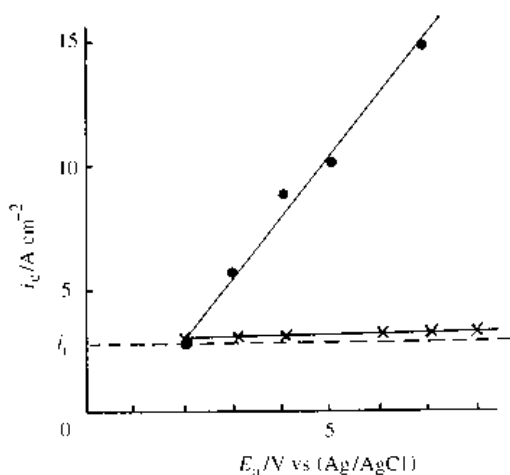


Fig. 2. Plots of current density,  $i_c$ , of anodic dissolution of a tungsten RDE in alkali at the end of the potential pulse against pulse amplitude,  $E_a$ , under the following conditions: in the pauses between the anodic pulses, (x) a potential of  $-0.7$  V (Ag/AgCl, sat. KCl) was applied, at which the current did not flow; (●) a cathodic potential  $E_c = 2$  V (Ag/AgCl, sat. KCl) was applied, which caused the hydrogen evolution;  $t_1 = t_2 = 1 \times 10^{-2}$  s.

several times by applying cathodic potential pulses in the pauses between the anodic pulses. This may be explained, first, by an increase of the near-electrode concentration,  $c_s$ , of hydroxyl ions due to cathodic hydrogen evolution, and secondly, by the fact that the bubbles of hydrogen evolving during the cathodic half-period stir the electrolyte in the near-electrode layer, thus reducing the concentration changes in the diffusion layer in the anodic half-period (i.e. increasing  $c_s$ ). Too intense gas evolution during the cathodic half-period may cause electrode surface shadowing in the anodic pulse and thus reduce the effect of the anodic dissolution intensification (Fig. 3).

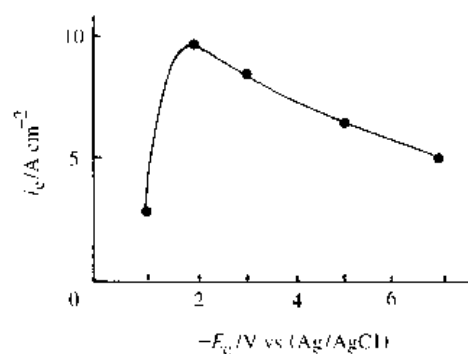


Fig. 3. Effect of amplitude,  $E_c$  of cathodic potential pulse on the current density,  $i_c$ , at the end of anodic potential pulse, at  $E_a = 5$  V (Ag/AgCl, sat. KCl) and  $t_1 = t_2 = 1 \times 10^{-2}$  s.

## 5. Conclusions

At pulse-on times  $t_1 = 2 \times 10^{-3}$  s and  $t_1 = 1 \times 10^{-1}$  s, and various pulse-off times  $t_2$  and at medium and high  $\gamma = t_1/(t_1 + t_2)$ , the measured pulse limiting currents  $i_{lp}$  of anodic dissolution of a tungsten rotating disc electrode in alkali (unipolar rectangular current pulses) are close to the  $i_{lp}$  values, calculated by Equations 5, 7 and 8. At  $\gamma = 1$ ,  $i_{lp}$  closely approaches the steady-state limiting current,  $i_l$ .

At low  $\gamma$ , the results of  $i_{lp}$  calculations by Equations 7 and 8 agree very closely and give  $i_{lp}$  values, which are higher than those calculated by Equation 5. In this case, the experimental data on pulse anodic dissolution of tungsten in alkali are better described by Equations 7 and 8. The deviation of calculated  $i_{lp}$  values from experimental values usually lies within 10%.

An average value of pulse limiting current  $\bar{i}_{lp}$  of tungsten dissolution in alkaline solutions increases with increase in  $\gamma$ , and at  $\gamma \rightarrow 1$ ,  $\bar{i}_{lp} \rightarrow i_l$ . The  $\bar{i}_{lp}$  value is higher for pulses of short duration ( $t_1 = 2 \times 10^{-3}$  s).

Application of bipolar potential pulses enhances the anodic dissolution of tungsten in alkali due to the hydrogen bubble evolution during the cathodic half-period; these bubbles stir the solution in the vicinity of the electrode and raise the anodic current. There is an optimal value of cathodic pulse amplitude for increasing the rate of tungsten dissolution under bipolar voltage pulses.

## Acknowledgement

This work was supported by the Russian Foundation for Fundamental Research, project 95-03-09844a.

## References

- [1] A. D. Davydov and J. Kozak, 'Vysokoskorostnoe Elektrokhimicheskoe Formoobrazovanie' ('High-rate Electrochemical Shaping'), Nauka, Moscow (1990) 272 pp.
- [2] S. Kh. Ait'yan, A. D. Davydov and B. N. Kabanov, *Soviet Electrochem.* **8** (1972) 1358.
- [3] V. S. Krylov, A. D. Davydov and V. N. Malienko, *ibid.* **8** (1972) 1422.
- [4] A. D. Davydov, V. S. Krylov and G. R. Engel'gart, *ibid.* **16** (1980) 163.
- [5] T. G. Rosebrugh and W. L. Miller, *J. Phys. Chem.* **14** (1910) 816.
- [6] A. M. Pesco and H. Y. Cheh, in 'Modern Aspects of Electrochemistry', No.19 (edited by B. E. Conway, J. O'M. Bockris, and R. E. White), Plenum Press, New York (1989) p. 251.
- [7] D. -T. Chin, 'Transport Processes in Electrochemical Systems' (edited by R. S. Yeo, T. Katan and D. -T. Chin), Electrochemical Society, Pennington, NJ (1982) 21.
- [8] N. Ibl, *Surf. Technol.* **10** (1980) 81.
- [9] *Idem*, *Metalloberflache* **33** (1979) 51.
- [10] D. -T. Chin, *J. Electrochem. Soc.* **130** (1983) 1657.
- [11] H. Y. Cheh, *ibid.* **118** (1971) 551.
- [12] M. Datta and D. Landolt, *Surf. Technol.* **25** (1985) 97.
- [13] C. C. Tang and C. C. Wan, *Mater. Chemi. Phys.* **24** (1990) 503.
- [14] D. -T. Chin, J. Y. Wang, O. Dossenbach, J. -M. Locarnini and A. Numanoglu, *Electrochim. Acta* **36** (1991) 625.
- [15] J. Y. Wang, D. Balamurugan, and D. -T. Chin, *J. Appl. Electrochem.* **22** (1992) 240.
- [16] K. Viswanathan, M. A. Farrell Epstein and H. Y. Chen, *J. Electrochem. Soc.* **125** (1978) 1772.